and more valid for outer-sphere than for inner-sphere transfers. The possibility of failure of (b) will probably rest on detailed mechanistic analysis in any given case. Finally, we would expect F to differ from unity most substantially when A and B are of very different charges or sizes, or when the solvent system is highly inhomogeneous (such as for membrane-bound species).

With these generalizations in mind, we might examine two of the standard cases for which the cross-relations in the forms (17) or (4) fail to hold. The first involves the reaction[6,9]

$$Ce^{IV} + Fe^{II} \rightarrow Ce^{III} + Fe^{III} \quad (18)$$

in aqueous solution. The cross-relations (4) predict its rate as 6×10^5 M^{-1} s^{-1}, whereas experimentally the rate is roughly 700 M^{-1} s^{-1}. Similarly, for the reaction of V^{III} with Cr^{III}, the observed rate is 60 times the calculated one,[6] and a large number of reactions of Co^{II}/Co^{III} are observed to show large deviations[6,10] from (4). Other well-documented cases include reactions between actinides.[11] Among the explanations suggested in the literature for these deviations are (1) changes in spin multiplicity; (2) substantial changes in the inner-sphere geometry; (3) formation of binuclear intermediates; (4) inner-sphere mechanisms for k_{12}, while outer-sphere behavior occurs for k_{11}, k_{22}; (5) atom transfer, as opposed to ET, as the actual mechanism.

Based on our simple thermodynamic arguments, both (1) and (2) may be dismissed as possible expanations: both of them are already included in the free energies of (13). If (3) occurs, our assumption (a) will break down, while if (4) holds both (a) and (b) will fail. Although a similar analysis in terms of thermodynamic cycles holds for atom-transfer reactions,[8] mixing atom transfer (for k_{12}) and ET (for k_{11} and k_{22}) will not yield (13). Generally, if the observed rate is larger than that calculated from (4), one would tend to blame (3), (4), or (5), while, if the converse is true, either (5) or (6) if Z_{AB}^2 differs considerably from $Z_{AA}Z_{BB}$ may be to blame. For (18) this might be so, since the Coulombic barrier against successful IV/III collisions should be substantially greater than that against II/III collisions.

We would like to remark on the difference between the Marcus f of (4) and F of (16). The Marcus expression derives specifically from his solvent dielectric model, in particular from his Gaussian-type form for the effective activation free energy. Our form, on the other hand, does not result from any microscopic model of the activation process. The expression (4) has the advantage of known form (given the exchange rates ΔG_{AB} and Z), but it does depend on a specific microscopic picture, which may fail (for instance, in the "abnormal", highly exoergic regime).[12] Expression (16) is more general, but, except for qualitative statements ("high charge and large bulk reduce Z"), it is difficult to make quantitative.

The Brønsted coefficient

$$\alpha = -\partial \ln (k_{AB}/z_{AB})/\partial(\Delta G_{AB}/RT) \quad (19)$$

is precisely $+1/2$ for our rate relationship (15). This predicts that the rate k_{AB} will continue to increase without limit as the reaction becomes more exoergic (that is as ΔG_{AB} becomes more negative). The Marcus form (4), on the other hand, predicts that the rate will start to decrease beyond a certain critical exoergicity; this high-exoergicity realm is often referred to as the inverted region. Other forms for k_{12} predict differing behavior in this region (slower falloff[12a] or constant[13]). We simply note that α *must* be $+1/2$ unless either (a) or (b) fails or one of (3-6) occurs. The most probable cause is the failure of (a); this has been remarked on previously[14] and modified forms involving the parameter α have been defined. One expects on general grounds[15] that $\alpha \approx 1/2$ for $\Delta G_{AB} \approx 0$, and that for $\Delta G_{AB} \ll 0$ α will be quite small with the transition state resembling the collision complex of the reactants; thus the activation is not independent, and (15) will fail.

Acknowledgments. We thank Noam Agmon for helpful remarks, and M.R. is grateful to M. D. Newton for incisive comments on electron-transfer theory.

(9) M. G. Adamson, F. S. Dainton, and P. Glentworth, *Trans. Faraday Soc.*, **61**, 689-701 (1965). Compare also R. A. Marcus and N. Sutin, *Inorg. Chem.*, **14**, 213-216 (1974).
(10) D. P. Rillema, J. F. Endicott, and R. C. Patel, *J. Am. Chem. Soc.*, **94**, 394-401 (1972).
(11) R. B. Fulton and T. W. Newton, *J. Phys. Chem.*, **74**, 1661-1669 (1970).
(12) E.g., S. F. Fischer and R. P. Van Duyne, *Chem. Phys.*, **26**, 9-16 (1977); D. Rehm and S. Weller, *Isr. J. Chem.*, **8**, 259-271 (1970); M. T. Indelli and F. Scandola, *J. Am. Chem. Soc.*, **100**, 7733-7734 (1978); J. Eriksen and C. Foote, *J. Phys. Chem.*, **82**, 2659-2962 (1978); J. K. Nagle, W. J. Dresseck, and T. J. Meyer, *J. Am. Chem. Soc.*, **101**, 3993-3995 (1979).
(13) N. Agmon and R. D. Levine, *Chem. Phys. Lett.*, **52**, 197-200 (1977).
(14) Cf., e.g., ref 1, p 135.
(15) R. W. Lumry and H. Eyring, *J. Phys. Chem.*, **58**, 110 (1954).

Matrix Photoionization and Radiolysis of Boron Trihalides. Infrared and Ultraviolet Spectra of BCl_3^+ and BBr_3^+ and Infrared Spectra of BCl_2 and BBr_2

J. Houston Miller and Lester Andrews*

Contribution from the Chemistry Department, University of Virginia, Charlottesville, Virginia 22901. *Received March 6, 1979*

Abstract: Infrared spectra of argon/boron trihalide mixtures deposited onto a cesium iodide window at 15 K with simultaneous proton radiolysis revealed boron isotopic absorptions for ν_4 and ν_5 of $HBCl_2$ and $HBBr_2$; isotopic splittings clearly show that ν_4 is the in-plane deformation and ν_5 is the antisymmetric $B-X_2$ stretching mode. Irradiation of boron trihalide samples with a windowless argon resonance lamp generated sharp infrared absorptions due to both boron isotopes of a new product on the high-energy side of the strong ν_3 parent absorptions. These bands, which disappeared on photolysis with a filtered high-pressure mercury arc, are assigned to the parent cations BCl_3^+ and BBr_3^+. Optical absorption spectra of similarly produced samples gave broad, photosensitive bands in the near-ultraviolet; these band positions agree with energy differences between bands in the photoelectron spectra. Both radiolysis and vacuum ultraviolet photolysis produced bihalide ions HX_2^- and boron isotopic absorptions just above the precursor absorptions which are assigned to ν_3 of BCl_2 and BBr_2. Boron isotopic data provides a $125 \pm 5°$ determination of the bond angles for these free radicals.

Introduction

The observation of small reactive halides of first-row elements has developed rapidly over the past decade through the use of matrix isolation spectroscopy. The matrix techniques discussed in this paper in addition to metal atom reactions have been used in studies of carbon,[1-7] nitrogen,[8-11] and oxygen[12-15] halides in this

0002-7863/80/1502-4900$01.00/0

and other laboratories. However, studies of analogous boron halide molecules have not kept pace with those of its first-row neighbors, although ultraviolet spectra of boron atoms and molecules,[16] infrared studies of borane,[17] boron halides,[18] and several other boron containing species,[19] and ESR observation of BF_2[20] have been reported. This paper describes the observation of two new boron halides: the triatomic radical BX_2, formed by radiolysis and photolysis, and the parent cation BX_3^+, formed by photoionization, which provides the first optical spectroscopic data on the boron dihalide radicals and trihalide cations.

Experimental Section

The proton beam apparatus and operating procedures have been described previously.[6] Research grade hydrogen (Matheson) was used as the beam gas, and currents of about 40 μA were measured at the sample for 2 keV protons. Samples of the boron trihalides in argon were deposited for 20 h onto a CsI window at 15 K while being bombarded with protons. Infrared spectra were recorded on a Beckman IR-12 filter-grating spectrophotometer during and after sample deposition. In some experiments, the matrix was cycled to about 35 K to allow sample diffusion and then recooled to 15 K for recording additional spectra. Wavenumber accuracy is ± 0.5 cm^{-1} for individual bands and ± 0.1 cm^{-1} within isotopic multiplets.

Boron trihalide samples were handled in a stainless steel vacuum manifold prepared by reacting BF_3 and BCl_3 (Matheson) gases with trace moisture in the system warmed to about 50 °C with heater tape overnight. The manifold was evacuated warm and then cooled to room temperature, and matrix samples of BF_3, BCl_3, and BBr_3 (Eastman Organic Chemicals) were prepared by using $Ar/BX_3 = 200/1$ and 400/1 concentrations. Impurity absorptions decreased in successive experiments as passivation of the system became more complete.

Matrix photoionization experiments were performed by using the 10-mm-i.d. quartz windowless argon resonance lamp and cryogenic equipment described in recent publications.[7,21] Several experiments were done with each trihalide involving the simultaneous deposition of the Ar/BX_3 mixture with vacuum ultraviolet radiation for 20-h periods; dilution of the sample by the discharged argon gave BX_3 concentrations in the matrix less than half of the initial concentration. Infrared spectra were recorded during and after sample deposition. Samples were then photolyzed with a water-filtered high-pressure mercury arc (Illumination Industries, Inc.) using colored glass filters to remove high-energy light (typical cutoffs were 420, 340, and 290 nm) in successive photolyses. The apparatus for argon resonance photolysis studies in optical experiments[21] was similar to that of the infrared studies. The sapphire sample window was maintained at 22 ± 2 K, and optical spectra were recorded on a Cary 17 spectrophotometer.

Results

Infrared and optical absorption studies following proton radiolysis and argon resonance photoionization of boron trihalide samples will be described.

Proton Radiolysis. BF_3. Three experiments were done with BF_3. The first study involved irradiation of an $Ar/BF_3 = 200/1$ mixture with protons for 21 h. In addition to the parent ν_3 antisymmetric stretching absorptions at 1445 cm^{-1} ($^{11}BF_3$) and 1496 cm^{-1} ($^{10}BF_3$) and numerous impurity bands between 1350 and 1480 cm^{-1} (mostly $B(OH)_3$,[22] a hydrolysis product of BF_3), a new band was observed at 1390 cm^{-1}. The next experiment involved the deposition of an identically prepared Ar/BF_3 mixture without proton radiolysis. All bands in the 1350–1500-cm^{-1} region with the exception of the 1390-cm^{-1} feature were reproduced in this experiment. The final experiment in this series was the deposition of an $Ar/BF_3 = 400/1$ sample with radiolysis. Again, the 1390-cm^{-1} band grew in with radiolysis and sample deposition.

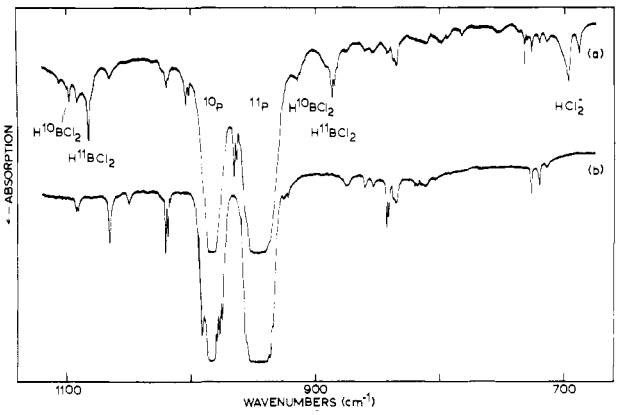

Figure 1. Infrared spectra of $Ar/BCl_3 = 200/1$ matrix samples deposited at 15 K: (a) sample condensed with simultaneous proton radiolysis for 20 h; (b) sample condensed without radiolysis. P denotes BCl_3 absorptions.

Table I. Product Absorptions (cm^{-1}) and Intensities (Absorbance Units) Observed in Proton Radiolysis and Argon Resonance Photolysis-Photoionization Experiments with Argon/Boron Trichloride Samples

radiolysis	photolysis	ident
696 (0.09)	696 (0.17)	HCl_2^-
731 (0.02)[a]	731 (0.02)	$^{11}BCl_2$
886 (0.09)[b]	886 (*c*)	$H^{11}BCl_2$
914 (0.025)		$H^{10}BCl_2$
965.9 (0.23)[a]	965.7 (0.24)	$^{11}BCl_2$
1004.5 (0.06)[a]	1004.3 (0.07)	$^{10}BCl_2$
1082.5 (0.20)[b]	1082 (*c*)	$H^{11}BCl_2$
1098.0 (0.05)[b]		$H^{10}BCl_2$
	1090.1 (0.30)[d]	$^{11}BCl_3^+$
	1132.5 (0.07)[d]	$^{10}BCl_3^+$

[a] Destroyed on sample warming. [b] Decreased on sample warming. [c] Observed in first photolysis experiment. [d] Destroyed by mercury arc photolysis.

BCl_3. Two radiolysis experiments were done with $Ar/BCl_3 = 200/1$ samples after the system was well passivated. Both experiments produced HCl_2^- at 696 cm^{-1}[24] (A = absorbance = 0.09 given for the more productive experiment), a weak doublet at 731, 728 cm^{-1} ($A = 0.02, 0.01$) indicated with an arrow in Figure 1, a partially resolved triplet at 886.3, 884.3, 882.3 cm^{-1} ($A = 0.09, 0.06, 0.01$), a weak 914.0, 912.0-cm^{-1} doublet ($A = 0.025, 0.015$), sharp doublets at 965.9, 963.5 ($A = 0.23, 0.14$) and 1004.5, 1002.0 cm^{-1} ($A = 0.06, 0.04$), and a sharp boron isotopic doublet at 1082.5, 1098.0 cm^{-1} ($A = 0.20, 0.05$) which are given in Table I; the 670–1120-cm^{-1} region in the radiolysis experiments is illustrated in Figure 1a. Sample warming to 35 ± 2 K to allow limited diffusion of trapped species reduced the sharp 886-cm^{-1} multiplet and 1098- and 1082-cm^{-1} bands by 50% and destroyed the 731- and 1005-cm^{-1} bands (966 cm^{-1} was not scanned). A final BCl_3 experiment was performed without radiolysis, and the above described radiolysis product bands were not observed as

(1) Milligan, D. E.; Jacox, M. E. *J. Chem. Phys.* **1968**, *48*, 2265.
(2) Andrews, L. *J. Chem. Phys.* **1968**, *48*, 972.
(3) Andrews, L.; Carver, T. G. *J. Chem. Phys.* **1968**, *49*, 896.
(4) Smith, D. W.; Andrews, L. *J. Phys. Chem.* **1972**, *76*, 2718.
(5) Jacox, M. E.; Milligan, D. E. *J. Chem. Phys.* **1971**, *54*, 3935.
(6) Andrews, L.; Grzybowski, J. M.; Allen, R. O. *J. Phys. Chem.* **1975**, *79*, 904.
(7) Prochaska, F. T.; Andrews, L. *J. Chem. Phys.* **1977**, *67*, 1091.
(8) Milligan, D. E.; Jacox, M. E. *J. Chem. Phys.* **1964**, *40*, 2461.
(9) Harmony, M. D.; Myers, R. J. *J. Chem. Phys.* **1962**, *37*, 636.
(10) Jacox, M. E.; Milligan, D. E. *J. Chem. Phys.* **1967**, *46*, 184.
(11) Minkwitz, R.; Froben, F. W. *Chem. Phys. Lett.* **1976**, *39*, 473.
(12) Arkell, A.; Reinhard, R. R.; Larson, L. P. *J. Am. Chem. Soc.* **1965**, *87*, 1016.
(13) Andrews, L.; Raymond, J. I. *J. Chem. Phys.* **1971**, *55*, 3078, 3087.
(14) Chi, F. T.; Andrews, L. *J. Phys. Chem.* **1973**, *77*, 3062.
(15) Tevault, D. E.; Walker, N.; Smardzewski, R. R.; Fox, W. B. *J. Phys. Chem.* **1978**, *82*, 2733.
(16) Graham, W. R. M.; Weltner, W., Jr. *J. Chem. Phys.* **1976**, *65*, 1516.
(17) Kaldor, A.; Porter, R. F. *J. Am. Chem. Soc.* **1971**, *93*, 2140.
(18) Bassler, J. M.; Timms, P. G.; Margrave, J. L. *J. Chem. Phys.* **1966**, *45*, 2704. Nimon, L. A.; Seshadri, K. S.; Taylor, R. C.; White, D. *Ibid.* **1970**, *53*, 2416.
(19) Lory, E. R.; Porter, R. F. *J. Am. Chem. Soc.* **1973**, *95*, 1766. Snelson, A. *High Temp. Sci.* **1972**, *4*, 318.
(20) Nelson, W.; Gordy, W. *J. Chem. Phys.* **1969**, *51*, 4710.
(21) Andrews, L.; Tevault, D. E.; Smardzewski, R. R. *Appl. Spectrosc.* **1978**, *32*, 157.
(22) Andrews, L. *J. Chem. Phys.* **1975**, *63*, 4465.
(23) Bethell, D. E.; Sheppard, N. *Trans. Faraday Soc.* **1975**, *51*, 9.
(24) Milligan, D. E.; Jacox, M. E. *J. Chem. Phys.* **1970**, *53*, 2034.

Table II. Product Absorptions (cm^{-1}) and Intensities (Absorbance Units) Observed in Proton Radiolysis and Argon Resonance Photolysis-Photoionization Experiments with Argon/Boron Tribromide Samples

radiolysis	photolysis	ident
596.6 (0.06)[a]		$^{11}BBr_2$
619.2 (0.015)[a]		$^{10}BBr_2$
673 (0.05)[b]		$^{10}BH_xBr_y$
699 (0.01)[b]		$^{11}BH_xBr_y$
729 (0.05)	729 (0.10)	HBr_2^-
768 (0.50)		$H^{11}BBr_2$
778 (0.15)		site?
793 (0.14)		$H^{10}BBr_2$
833.1 (0.68)[a]	833 (0.08)	$^{11}BBr_2$
870.1 (0.17)[a]	870 (0.02)	$^{10}BBr_2$
930 (0.01)	930.3 (0.30)[c]	$^{11}BBr_3^+$
	970.9 (0.08)[c]	$^{10}BBr_3^+$
	978 (0.04)	?
980 (0.09)[b]		$^{11}BH_xBr_y$
984 (0.03)[b]		$^{10}BH_xBr_y$
1032 (0.58)		$H^{11}BBr_2$
1042 (0.20)		$H^{10}BBr_2$

[a] Decreased substantially (70%) on sample warming. [b] Increased markedly (×6) on sample warming. [c] Destroyed on mercury arc photolysis.

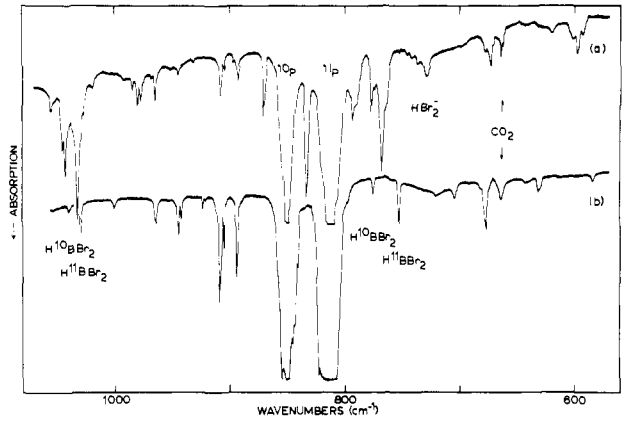

Figure 2. Infrared spectra of argon/boron tribromide matrix samples: (a) Ar/BBr_3 = 400/1 sample deposited at 15 K with proton beam radiolysis; (b) Ar/BBr_3 = 200/1 sample deposited without radiolysis. P denotes BBr_3 absorptions.

can be seen by comparison of the spectra in Figure 1. The present BCl_3 matrix spectra include impurity features at 720, 726, 811, 835, 875, 1020 (triplet), and 1145 cm^{-1}, as well as the $B(OH)_3$ system between 1350 and 1480 cm^{-1} and HCl near 2890 cm^{-1}. These impurity absorptions decreased in the series of experiments as passivation of the vacuum manifold for handling BCl_3 became more complete.

BBr_3. Three experiments were done with BBr_3: (a) Ar/BBr_3 = 200/1 with radiolysis, (b) Ar/BBr_3 = 200/1 with no radiolysis, and (c) Ar/BBr_3 = 400/1 with proton-beam radiolysis. Bands observed in the 200/1 experiment were exactly reproduced in the later, more dilute trial. New absorptions produced by radiolysis in the region of interest were a doublet at 596.6 (A = 0.06), 619.2 (0.015), 673, 729, 768, 778, 793 cm^{-1}, a doublet at 833.1 (0.70), 870.1 (0.18) cm^{-1}, a weak 930 (0.01) cm^{-1} feature, and bands at 1032 and 1042 cm^{-1}, given in Table II, in addition to BBr_3 parent absorptions at 812.7 and 849.2 cm^{-1}, which are denoted P in the spectrum of Figure 2a. The 729-cm^{-1} absorption is due to HBr_2^- which has been observed in earlier studies.[25] Sample warming to allow limited diffusion reduced the 768, 793- and 1032, 1042-cm^{-1} doublets by 40% and the 596-, 619-, and 871-cm^{-1} bands by 70% (834 cm^{-1} was not scanned) and destroyed the weak 930-cm^{-1} band, while boron isotopic doublets at 673, 699 and 979, 984 cm^{-1} increased sixfold. The spectrum of a BBr_3 matrix sample

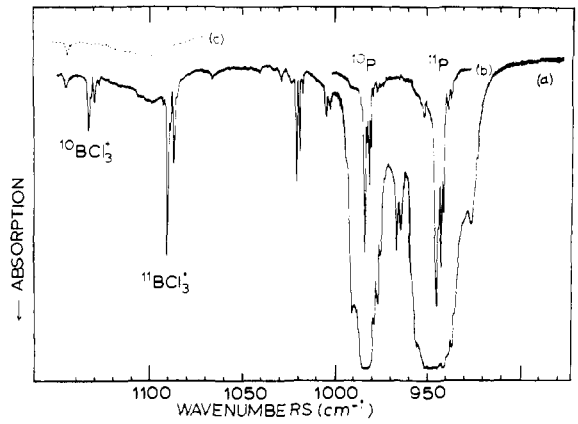

Figure 3. Infrared spectra of the products of windowless argon resonance photolysis of a 200/1 sample of BCl_3 in solid argon: (a) high-resolution of parent ν_3 absorption region after 20 h of photolysis; (b) trace of parent ν_3 absorption after only 20-min sample deposition; (c) product region after 30 min of 290–1000-nm photolysis. Argon from discharge diluted the sample to approximately 400/1.

without radiolysis is shown in Figure 2b; impurity bands were observed at 892 cm^{-1}, boron isotopic features at 907, 944 and 964, 1000 cm^{-1}. Sharp boron isotopic doublets at 752.5, 775.0 (A = 0.28, 0.07) and 1030.0, 1040.0 cm^{-1} (A = 0.20, 0.06) are in agreement with the gas-phase spectrum of $HBBr_2$,[26] and this molecule could be an impurity in the present sample.

Photoionization. BF_3. Two experiments were done with BF_3; no bands were seen in experiments involving the simultaneous condensation of the sample mixtures with argon discharge photolysis that were not also observed in similar experiments with no photolysis.

BCl_3. Four experiments were done with Ar/BCl_3 = 200/1 samples; final infrared spectra of photolysis products revealed impurity bands also observed in the blank experiment illustrated in Figure 1b, which decreased relative to BCl_3 precursor absorptions in the series of BCl_3 studies. The first argon discharge photoionization experiment produced new bands at 696 (A = 0.40), 731 (0.02), 886 (0.02), 965.7, 963.3 (A = 0.24, 0.15 doublet), 1004.3, 1001.9 (A = 0.07, 0.04 doublet), 1082 (A = 0.04), 1090 (0.13), 1098 (0.01), 1132 cm^{-1} (0.04). Photolysis with 420–1000-nm light reduced the 1090- and 1132-cm^{-1} bands by 10% and the full arc destroyed the 1090- and 1132-cm^{-1} bands without affecting the other product absorptions. A second experiment gave similar results. After continued passivation of the BCl_3 manifold for two additional days, the spectrum from the third experiment, which is illustrated in Figure 3 and listed in Table I, gave reduced impurity absorptions, reduced HCl_2^- at 696-cm^{-1}, no absorptions at 886 and 1083 cm^{-1}, the sharp doublets 1004.3, 1001.9 and 965.7, 963.3 cm^{-1} on the side of the strong BCl_3 absorptions, the weak 731-cm^{-1} band, and increased absorption at 1090.1 cm^{-1} (A = 0.30 multiplet) and 1132.5 cm^{-1} (A = 0.07 multiplet). Upon photolysis with mercury arc light between 290 and 1000 nm, the 696-, 731-, 965-, and 1004-cm^{-1} bands were unchanged in intensity, while the 1090- and 1132-cm^{-1} bands were destroyed. A second photolysis with the full arc failed to change the 696-, 731-, 965-, and 1004-cm^{-1} bands. Figure 3a shows the spectral region near the parent ν_3 mode, and the dashed trace, Figure 3c, shows the same region after 30 min of 290–1000-nm photolysis. Also shown is the parent ν_3 mode of $^{10}BCl_3$ (984.0-cm^{-1}) and $^{11}BCl_3$ (946.0-cm^{-1}) in the same experiment after sample condensation for 20 min (Figure 3b), demonstrating similarities in the isotopic splittings and intensities for the parent and product multiplets. Under higher resolution the product band was resolved to 1090- (A = 0.30), 1088.5- (A = 0.04), 1086.6- (A = 0.08), and 1085-cm^{-1} (A = 0.03 shoulder) features. In a final infrared experiment using 10% Kr doped Ar discharge photoionization, the only product band was 1090 cm^{-1} (A = 0.03).

(25) Milligan, D. E.; Jacox, M. E. *J. Chem. Phys.* **1971**, *55*, 2550.

(26) Wason, S. K.; Porter, R. F. *J. Phys. Chem.* **1965**, *69*, 2461.

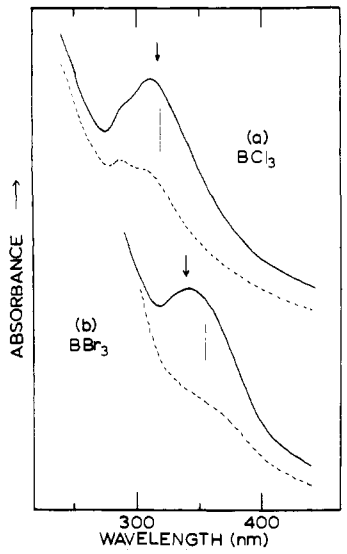

Figure 4. Near-ultraviolet absorption spectra of the products of windowless argon resonance photolysis of BX_3: (a) $Ar/BCl_3 = 200/1$; (b) $Ar/BBr_3 = 200/1$. Dashed traces recorded after 30 min of 290–1000-nm photolysis. Argon from discharge diluted sample to approximately 400/1. Arrows denote absorption band positions deduced from photoelectron spectra; vertical lines inside bands indicate center of integrated absorption.

A boron trichloride/argon sample was codeposited at 0.7 mM/h for 4 h with argon resonance radiation in an optical absorption study. Final spectra revealed a broad band centered at 320 nm, which is shown in Figure 4a. Photolysis with 340–600-nm radiation for 30 min halved the absorption and a like exposure to 290–1000-nm radiation nearly destroyed the band, as shown in the dashed trace in the figure. This new absorption was not observed in a BCl_3 blank experiment without photoionization.

BBr_3. Argon/BBr_3 mixtures (200/1) were photolyzed by the windowless argon lamp during condensation in four experiments. Product bands were observed at 729, 833 ($A = 0.08$), 870 (0.02), 930.3 (0.30), and 970.9 cm^{-1} (0.08) that were not seen in the blank experiment. Numerous other bands seen in both photoionization and blank experiments, include the strong $^{10}BBr_3$ and $^{11}BBr_3$ ν_3 modes at 849.2 and 812.7 cm^{-1}, a band at 892 cm^{-1}, sharp doublets at 908 and 945 cm^{-1}, and weaker bands at 964, 977, and 1000 cm^{-1}.

The 930- and 970-cm^{-1} product bands were stable to photolysis by 420–1000-nm light, decreased one-third with 340–600-nm photolysis, halved by 290–1000-nm radiation and virtually destroyed with 30 min of mercury arc photolysis using no high-energy filter (220–1000 nm passed). The 729-, 833-, and 870-cm^{-1} product bands remained constant throughout the photolysis studies. Figure 5 shows a representative BBr_3 spectrum with dashed lines illustrating the unfiltered photolysis scan. A final infrared experiment with 10% Xe doped Ar discharge radiation photolysis gave broad 833- and 870-cm^{-1} bands ($A = 0.08, 0.02$), a broad 728-cm^{-1} feature ($A = 0.08$), and a broad 1030–1040-cm^{-1} absorption.

A 200/1 mixture of BBr_3 in argon was deposited over a 3-h period with argon resonance radiation for ultraviolet examination. A broad band centered at 355 nm was decreased substantially with 340–600-nm photolysis and was nearly destroyed by Pyrex-filtered photolysis (290–1000 nm), as shown in Figure 4b. The band was not observed in a similar experiment without the argon resonance lamp.

Discussion

Major product species from matrix radiolysis and photoionization of boron trihalides will be identified and the matrix chemistry and bonding will be discussed.

Identification. Although the proton beam has sufficient energy (2 keV) for all simple molecular fragmentation processes, previous studies with CCl_4 and CBr_4 have shown that the major product

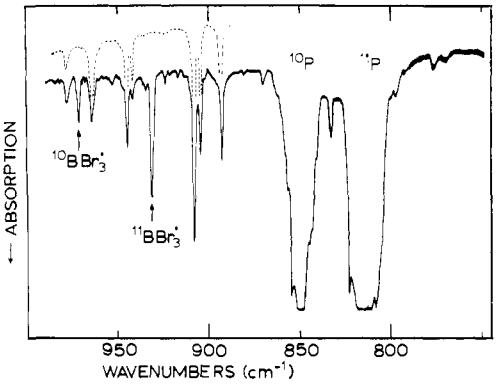

Figure 5. Infrared spectrum of the ν_3 region of BBr_3 ($Ar/BBr_3 = 200/1$) after 20 h of deposition at 15 K with simultaneous vacuum ultraviolet photolysis. The dashed trace was recorded after 30 min of 220–1000-nm photolysis. Argon from discharge diluted the sample to approximately 400/1.

absorptions are the free radicals CCl_3 and CBr_3 formed by the dissociation of a single carbon–halogen bond.[6] The matrix radiolysis of BX_3 precursors is, therefore, expected to give the BX_2 radical as a major product. Experiments with deuteron radiolysis of Cl_2 and O_2 have produced DCl_2^- and DO_2, which shows that the bombarding particle can become involved in the matrix chemistry.[27] On the other hand, argon resonance photolysis and photoionization is more selective, and experiments with CCl_4 and CBr_4 have produced CCl_3^+ and CBr_3^+ as major products, probably arising from the unstable CCl_4^+ and CBr_4^+ parent cations; smaller yields of the CCl_3 and CBr_3 radicals were also produced.[7] Comparison of the earlier carbon–halogen studies using these two techniques for producing transient species will be helpful for identification of the new boron–halogen species.

HBX_2. The only product in the boron–halogen studies that can be identified from earlier gas-phase infrared spectra of boron–halogen compounds is HBX_2, which is a major product in the radiolysis experiments. The two strongest bands in the spectrum of gaseous $HBCl_2$ at 1089 and 892 cm^{-1} have been assigned to ν_4 and ν_5 and designated antisymmetric B–Cl stretch and in-plane deformation modes, respectively; unfortunately, the ^{10}B counterparts could not be accurately determined due to overlapping of bands.[28] In a later matrix study, boron isotopic shifts of 17 and 22 cm^{-1}, respectively, were determined for these bands[29] although the absolute wavenumber accuracy is subject to question. The proton radiolysis experiments with BCl_3 produced boron isotopic bands at 1082.5, 1098.0 cm^{-1} ($A = 0.20, 0.05$) and multiplets at 886, 914 cm^{-1} ($A = 0.09, 0.025$) with relative intensities in excellent agreement with the natural abundance of boron isotopes (80.4% ^{11}B, 19.6% ^{10}B) and intensity measurements on BCl_3 precursor absorptions. The 886-cm^{-1} band is a partially resolved triplet at 886.3, 884.3, 883.3 cm^{-1} ($A = 0.09, 0.06, 0.01$) with appropriate relative intensities for two equivalent chlorine atoms with natural abundance chlorine isotopes (75.5% ^{35}Cl, 24.5% ^{37}Cl); the weaker 914-cm^{-1} feature is composed of a doublet at 914.0, 912.0 cm^{-1} ($A = 0.025, 0.015$). The strongest argon matrix bands at 1083 and 886 cm^{-1} are in sufficient agreement with the gas-phase spectrum of $HBCl_2$ to identify these present absorptions as $HBCl_2$. The isotopic splittings also confirm the assignment and provide a more accurate description of the normal modes.

The sharp 1082.5-cm^{-1} band (FWHM = 1.6 cm^{-1}) exhibits no chlorine isotopic splittings whereas the 886-cm^{-1} triplet clearly denotes a vibration of two equivalent chlorine atoms. The boron isotopic shift for the 886-cm^{-1} multiplet, 27.7 cm^{-1}, is slightly less than the 38.0-cm^{-1} splitting for the antisymmetric B–Cl stretching mode in BCl_3 whereas the 15.5-cm^{-1} boron isotopic shift for the

(27) Andrews, L.; Ault, B. S.; Grzybowski, J. M.; Allen, R. O. *J. Chem. Phys.* **1975**, *62*, 2461.
(28) Bass, C. D.; Lynds, L.; Wolfram, T.; DeWames, R. E. *J. Chem. Phys.* **1964**, *40*, 3611.
(29) Bass, C. D.; Lynds, L.; Wolfram, R.; DeWames, R. E. *Inorg. Chem.* **1964**, *3*, 1063.

sharp 1082.5-cm^{-1} band is slightly more than might be expected for an in-plane B–H deformation mode. Clearly, the two normal modes ν_4 and ν_5 (b_1) in $HBCl_2$ are mixed internal coordinates, but the isotopic splittings show that the ν_5 mode (886 cm^{-1}) has substantially more B–Cl stretching character and the ν_4 mode (1082 cm^{-1}) has substantially more H deformation character, and these modes must be designated accordingly.

Sharp, weak bands in the blank BBr_3 experiment at 1030, 1040 and 753, 775 cm^{-1} may be identified as $HBBr_2$ by comparison with the strong gas-phase bands[26] at 1040 and 775 cm^{-1}. Proton radiolysis produces strong, broader boron isotopic doublets at 1032, 1042 and 768, 792 cm^{-1} which are probably due to $HBBr_2$ produced by proton radiolysis with incorporation of the thermalized and neutralized proton into the product molecule or reaction of H atoms produced by radiolysis of hydrogen-containing impurities. The 1390-cm^{-1} product band in BF_3 radiolysis experiments is in sufficient agreement with the 1402 cm^{-1} gas-phase antisymmetric B–F stretching mode of HBF_2[30] to identify this product in BF_3 experiments.

A major product in proton radiolysis of BX_3 matrix samples is thus identified as the HBX_2 molecule. This suggests that the BX_2 radical is produced in these experiments and that HBX_2 is formed by the free radical reaction of H with BX_2 during sample condensation.

BX_2 Free Radicals. Two products common to the radiolysis and vacuum ultraviolet photolysis experiments are the HCl_2^- and HBr_2^- ions[24,25] and new boron isotopic doublets in BCl_3 studies at 966 and 1004 cm^{-1} and in BBr_3 experiments at 833 and 870 cm^{-1}. Observation of the bihalide ions shows that some precursor dissociation occurs in these experiments. The new doublets are assigned to the BCl_2 and BBr_2 free radicals for the following reasons. First, the doublets exhibit the 4/1 relative intensity ratio expected for a vibration involving a single boron atom. Second, in the BCl_3 studies, each band is resolved into a 3/2 relative intensity doublet with a 2.4-cm^{-1} separation; this denotes a vibration of two equivalent chlorine atoms (the 37–37 counterpart was obscured by overlapping BCl_3 absorptions). Third, these bands were not affected by mercury arc photolysis. Fourth, sample warming to allow limited diffusion of trapped species reduced these bands substantially more than the HBX_2 absorptions which is consistent with a reactive species. Finally, the BF_2 free radical has been detected in BF_3 matrix samples following radiolysis,[20] which supports the observation of BCl_2 and BBr_2 in these experiments.

The bands assigned to BCl_2 and BBr_2, respectively, at 966 and 833 cm^{-1} are near the antisymmetric B–X stretching modes of the BX_3 precursors and the HBX_2 molecules. The boron isotopic shifts for the strong BCl_2 and BBr_2 absorptions are 38.5 and 37.0 cm^{-1}, respectively, which are just 0.5 cm^{-1} higher than the boron shifts for the ν_3 modes of BCl_3 and BBr_3. The intensity, position, and boron isotopic shift show that the 966- and 833-cm^{-1} bands are due to ν_3 of $^{11}BCl_2$ and $^{11}BBr_2$, respectively.

The valence bond angle can be calculated from isotopic ν_3 fundamentals for symmetrical triatomic molecules. This procedure gives a lower limit when central atom isotopic ν_3 values are used and an upper limit with terminal atom isotopic ν_3 values.[31] The calculation gives angles of 115 ± 5° for BCl_2 and 116 ± 5° for BBr_2. Consideration of the 100–111° lower limit–upper limit calculations[32] for CCl_2 and the 108–124° limits[33] for O_3 (116.8°) shows that the valence angles for BCl_2 and BBr_2 are approximately 125 ± 5°. This predicts a slightly larger angle than the 120° value for the trihalides, which may be expected owing to removal of a halogen atom and its repulsions for the two remaining halogens. The angles estimated for BCl_2 and BBr_2 from isotopic ν_3 data are intermediate between the 112° value deduced from the 2s character of the unpaired electron in BF_2 from coupling of the B nuclear spin with the electron spin[20] and the 131° value for BH_2 determined from the high-resolution optical spectrum.[34]

Observation of the strong ν_3 (antisymmetric B–X) modes for BCl_2 and BBr_2 suggests that the weaker ν_1 (symmetric B–X) modes should also be found in the spectra. The symmetric B–Cl stretching mode for gaseous[28] $H^{11}BCl_2$ has been reported at 740 cm^{-1} so this region is appropriate for ν_1 of BCl_2; the difference between the ν_3 modes for BCl_2 and BBr_2 predicts that ν_1 of BBr_2 will be approximately 130 cm^{-1} lower than ν_1 for BCl_2. The radiolysis experiments with BBr_3 produced a sharp 596.6-cm^{-1} band (A = 0.060) and a weaker 619.2-cm^{-1} band (A = 0.015) which decreased substantially on sample warming. The boron isotopic shift is appropriate for the ν_1 mode of BBr_2. The BCl_3 radiolysis spectrum in Figure 1a shows a sharp 731-cm^{-1} band (A = 0.02) with a 728-cm^{-1} sideband (A = 0.01) which were destroyed on sample warming; the 731-cm^{-1} absorption is probably due to ν_1 of the $^{11}B^{35}Cl_2$ radical. The larger separation between the ν_3 and ν_1 modes for BCl_2 as compared to CCl_2 (ν_3 = 746 cm^{-1}, ν_1 = 720 cm^{-1})[35] and BBr_2 as compared to CBr_2 (ν_3 = 641 cm^{-1} ν_1 = 595 cm^{-1})[3] is a consequence of the larger valence angle in the boron dihalide radicals which allows more stretch–stretch interaction between the two bonds involved.

Parent Cations. The ionization energies of BF_3, BCl_3, and BBr_3 are 15.5, 11.6, and 10.5 eV, respectively.[36] The most intense 11.6- and 11.8-eV lines in the argon resonance lamp[21] are capable of photoionization of all the boron trihalides, except BF_3, during condensation with argon. Minor product features in the BCl_3 and BBr_3 photoionization experiments at 697 and 729 cm^{-1} are due to HCl_2^- and HBr_2^-, respectively;[24,25] observation of these anions indicates that photoionization occurs in these experiments. The bihalide ions are probably formed in these studies by reaction of the hydrogen halide, from hydrolysis of BX_3, with a halide ion, from electron capture by a halogen atom dissociation product. The bihalide ions (and undetected halide ions) provide the necessary charge balance for the trapping of isolated cations in these samples.

The product multiplets at 1090 and 1132 cm^{-1} in the BCl_3 experiment bear a striking resemblance to the $^{11}BCl_3$ and $^{10}BCl_3$ precursor absorptions recorded after 20 min of sample deposition (Figure 3). This multiplet has been analyzed in detail and the 9/1/3/1 relative intensity multiplet is due to the doubly degenerate vibration of three equivalent chlorine atoms with chlorine isotopes in natural abundance.[37] The relative intensities (A = 0.30 and 0.07, respectively) and shift between the 1090- and 1132-cm^{-1} absorptions denote a single boron atom species in agreement with the natural abundance of boron isotopes. The isotopic ratio 1132.5/1090.1 = 1.0389 for the new product band is in very good agreement with the ratio for ν_3 of the precursor, 984.0/946.0 = 1.0402. Thus, the isotopic data identify a new species of formula BCl_3.

The 1090- and 1132-cm^{-1} product multiplets are due to a photosensitive species; the absorptions were markedly decreased by 340–600-nm light and destroyed by 290–1000-nm photolysis. Comparison of the 12.3-eV appearance potential[38] of BCl_2^+ from BCl_3 with the precursor ionization energy of 11.6 eV indicates that the BCl_3^+ parent ion requires less than 1 eV to eliminate a chlorine atom at threshold and suggests that its photodissociation might proceed through some electronic state above threshold. The infrared multiplets at 1090 and 1132 cm^{-1} are, accordingly, assigned to the photosensitive $^{11}BCl_3^+$ and $^{10}BCl_3^+$ cations, respectively. The boron isotopic ratios show that the vibration is ν_3, the antisymmetric B–Cl stretching mode.

The ultraviolet spectrum of a BCl_3 sample subjected to argon resonance photoionization revealed a broad product absorption

(30) Porter, R. F.; Wason, S. K. *J. Phys. Chem.* **1965**, *69*, 2208.
(31) Allavena, M.; Rysnik, R.; White, D.; Calder, V.; Mann, D. E. *J. Chem. Phys.* **1969**, *50*, 3399.
(32) Hatzenbuhler, D. A.; Andrews, L.; Carey, F. A. *J. Am. Chem. Soc.* **1975**, *97*, 187.
(33) Andrews, L.; Spiker, R. C., Jr. *J. Phys. Chem.* **1972**, *76*, 3208.
(34) Herzberg, G.; Johns, J. W. C. *Proc. R. Soc. London, Ser. A* **1967**, *298*, 145.
(35) Andrews, L. *J. Chem. Phys.* **1968**, *48*, 979.
(36) Rosenstock, H. M.; Draxl, K.; Steiner, B. W.; Herron, J. T. *J. Phys. Chem. Ref. Data, Suppl.* **1977**, *6* (1).
(37) Comeford, J. J.; Abramowitz, S.; Levin, I. W. *J. Chem. Phys.* **1965**, *43*, 4536.
(38) Dibeler, V. H.; Walter, J. A. *Inorg. Chem.* **1969**, *8*, 50.

centered at 320 nm. This band exhibited similar photolysis behavior with the infrared multiplets, which links the IR and UV absorptions to the same molecular species and indicates assignment of the 320-nm absorption to BCl_3^+ as well. The photoelectron spectrum (PES) of BCl_3 consists of bands peaked at 11.73, 12.39, 12.66, 14.42, 15.54, and 17.7 eV.[39] The energy difference between the onset of the first band at 11.64 eV (adiabatic IP), assigned to ionization from the $1a_2'$ orbital, and the 15.54-eV peak, assigned to the 2e' orbital, is 3.90 eV, which corresponds to a dipole-allowed transition at 318 nm from the ground state of BCl_3^+. This excellent agreement with the 320-nm argon matrix band center confirms the observation of BCl_3^+ in the present experiments and shows that minimal geometry change occurs on ionization of BCl_3 to the $1a_2'$ ground state of BCl_3^+ since similar Franck–Condon factors govern both ionization and absorption to the common 2e' state of BCl_3^+.

The boron isotopic doublet at 930 and 970 cm^{-1} in BBr_3 photoionization experiments is due to a photosensitive species and BBr_3^+ is suggested by the above evidence for BCl_3^+. The boron isotopic ratio of the product doublet 970.9/930.3 = 1.0436 is in very good agreement with the parent ratio 849.2/812.7 = 1.0449. The ultraviolet spectrum of a BBr_3 sample subjected to ionizing radiation contained a strong, broad absorption centered at 357 nm that photolyzed with 290–1000-nm light. Similarly, the difference between the adiabatic first ionization, approximately 10.55 eV, and the vertical 14.20-eV peak in the PES[39] of BBr_3 corresponds to an electronic transition for the BBr_3^+ molecular ion. Again, the energy difference 3.65 eV (340 nm) is in very good agreement with the observed absorption centered at 355 nm which confirms the matrix observation of BBr_3^+. A like correspondence has been found for matrix absorptions of $CH_2X_2^+$ and chlorofluoromethane parent ions and their respective PES.[40,41]

The photophysical processes in these studies merit comment. Photodissociation of BCl_3^+ and BBr_3^+ presumably proceeds by halogen atom elimination giving BCl_2^+ and BBr_2^+, although the latter species have not been detected on photolysis. The mechanism for dissociation probably involves a dissociative $^2E'$ state; however, excitation to a bound $^2E'$ state followed by internal conversion to excited vibrational levels of the ground $^2A_2'$ state would surely give dissociation. The more complete photodissociation of BCl_3^+ with 290–1000-nm radiation as compared to BBr_3^+ is probably due to the argon matrix cage retaining the larger bromine atom. A similar effect has been encountered in the photodissociation of CCl_4^+ and CBr_4^+ in solid argon.[7]

The absorbance of BCl_3^+ relative to the BCl_3 precursor is relatively low in these experiments as compared to halocarbon precursors.[7] The strong 11.6–11.8-eV argon resonance lines in the windowless resonance lamp[21] are sufficiently energetic to ionize BCl_3 (IP = 11.6 eV); however, when krypton is doped into the argon discharge gas, most of the microwave energy pumps the krypton excited state at 10.0 eV which accounts for a substantially reduced yield of BCl_3^+ with krypton/argon discharge radiation. Likewise, the xenon resonance radiation from a xenon/argon discharge[21] (8.4 eV) is not sufficiently energetic to ionize BBr_3 (IP = 10.5 eV) which can be accomplished by argon resonance radiation. Even though there is some radiation in the 13–15-eV region in the argon plasma[21] and matrix solvation will red-shift ionization of BF_3 (IP = 15.5 eV), BF_3^+ could not be detected in these experiments.

Bonding. Boron trifluoride is a textbook example of the molecular orbital model for trigonal-planar molecules.[42] π bonding contributes to the strength of the boron–halogen bond in the BX_3 molecules, although π bonding to boron decreases with increasing halogen p-orbital size.[43,44] The ν_3 absorptions of the BCl_2 and BBr_2 radicals are sufficiently close to the ν_3 modes of the BX_3 precursor to infer that similar π bonding participates in the radical fragments as well, a point substantiated by approximate force-constant calculations for BX_2 and BX_3 using the ν_1 and ν_3 modes.

Table III. Comparison of Boron–Halogen and Carbon–Halogen Antisymmetric Stretching modes (cm^{-1}) for Neutral Molecules and Cations in Solid Argon

	Cl	Br	ref
$^{11}BX_3^+$	1090	930	this work
$^{11}BX_3$	946	813	this work
CX_3^+	1037	874	5–7
CX_3	898	773	2, 3
CX_2^+	1197	1019	47
$^{11}BX_2$	966	833	this work
CX_2	746	641	3, 35
HCX_2^+	1045	897	40
$H^{11}BX_2$	886	768	this work
HCX_2	900	786	40

Two other comparisons are noteworthy. First, the antisymmetric C–X stretching fundamentals of the HCX_2 free radicals are very near the HBX_2 molecule B–X stretching values as shown in Table III. Since π bonding surely contributes to the strength of the B–X bonds in HBX_2, it can be inferred that π bonding also contributes to the electronic stabilization in the HCX_2 free radicals, as proposed earlier from comparison of carbon–halogen stretching force constants.[45,46] Second, the antisymmetric stretching fundamentals of the BX_2 radicals are substantially higher (~220 cm^{-1}) than CX_2 values while the symmetric stretching modes are nearly the same. This comparison shows that any π bonding in the dihalocarbenes is substantially less than in the boron analogues, which reinforces the earlier conclusion from force constant comparisons that π bonding in CCl_2 and CBr_2 makes no measurable contribution to their vibrational potential functions.[3,35]

Perhaps the most interesting aspect of this work is the substantial increase in ν_3 of BCl_3^+ compared to BCl_3 (144 and 149 cm^{-1} for the two boron isotopic species) and for ν_3 of BBr_3^+ relative to BBr_3 (118 and 122 cm^{-1}). Ionization removes a nonbonding in-plane lone-pair a_2' electron from the halogen[40] and, from the agreement between the absorption spectrum and the PES band difference, causes minimal change in geometry. This vacancy on chlorine may facilitate contraction of the chlorine 3p orbital and make Cl_{3p}–B_{2p} π bonding more favorable in the cation than in the neutral molecule. Hence the increase in ν_3 vibrational energy for the cation may be attributed to increased π bonding in the cation. A marked increase in ν_3 for CCl_2^+ (1197 cm^{-1}) relative to CCl_2 (746 cm^{-1}) has been rationalized, in part, by the same mechanism.[47] A similar argument can be made for increased π bonding in BBr_3^+.[48] The increases in ν_3 for CCl_3^+ over CCl_3 (139 cm^{-1}), and CBr_3^+ over CBr_3 (101 cm^{-1}),[2,7] are strikingly similar to the BCl_3 and BBr_3 cases compared in Table III. This has been rationalized on the basis of removal of an antibonding π electron with a corresponding increase in π bonding in the CX_3^+ cation, which is isoelectronic with BX_3. Since the CCl_3 radical is nonplanar[49] and CCl_3^+ is surely planar, some geometry change follows ionization, which contrasts BCl_3 and BCl_3^+ where ion and neutral appear to have the same geometry.

Conclusions

Boron trihalides have been subjected to matrix radiolysis and photoionization during condensation with excess argon at 15 K.

(39) Potts, A. W.; Lempka, H. J.; Streets, D. G.; Price, W. C. *Philos. Trans. R. Soc. London, Ser. A* **1970**, *268*, 59. Bassett, P. J.; Lloyd, D. R. *J. Chem. Soc. A* **1971**, 1551.
(40) Andrews, L.; Prochaska, F. T.; Ault, B. S. *J. Am. Chem. Soc.* **1979**, *101*, 9.
(41) Andrews, L.; Prochaska, F. T. *J. Phys. Chem.* **1979**, *83*, 368.
(42) Gray, H. B. "Electrons and Chemical Bonding"; W. A. Benjamin: New York, 1965.
(43) Cotton, F. A.; Leto, J. R. *J. Chem. Phys.* **1959**, *30*, 993.
(44) Pauling, L. "The Nature of the Chemical Bond", 3rd ed.; Cornell University Press: Ithaca, New York, 1960.
(45) Carver, T. G.; Andrews, L. *J. Chem. Phys.* **1969**, *50*, 4223, 4235.
(46) Andrews, L.; Smith, D. W. *J. Chem. Phys.* **1970**, *53*, 2956.
(47) Andrews, L.; Keelan, B. W. *J. Am. Chem. Soc.* **1979**, *101*, 3500.
(48) It is for this reason that the photosensitive bands cannot be due to BCl_3^-. The anion electron would be antibonding (and probably depress the species from planarity) and reduce the ν_3 mode below the neutral BCl_3 value.
(49) Maass, G.; Maltsev, A. K.; Margrave, J. L. *J. Inorg. Nucl. Chem.* **1973**, *35*, 1945.

New boron isotopic absorptions in radiolysis and photoionization experiments just above the parent ν_3 modes are attributed to the BCl_2 and BBr_2 free radicals owing to the resolved chlorine isotopic splittings and the decrease on sample warming. Calculations based on boron isotopic ν_3 values predict 125 ± 5° valence angles for BCl_2 and BBr_2. Photoionization studies revealed boron isotopic doublets above the parent absorption which are assigned to ν_3 of BCl_3^+ and BBr_3^+; the BCl_3^+ absorptions exhibited multiplet structure appropriate for a doubly degenerate vibration of three equivalent chlorine atoms. These bands are photosensitive as expected from appearance potential data. Absorption bands at 320 and 357 nm in the ultraviolet are assigned to BCl_3^+ and BBr_3^+, in excellent agreement with the appropriate electronic band spacing in photoelectron spectra. The substantial increase in ν_3 of BCl_3 and BBr_3 on ionization, also characteristic of carbon–halogen systems, is attributed to increased π bonding in the cations.

Acknowledgments. The authors gratefully acknowledge financial support for this research from the National Science Foundation under Grant CHE 76-11640.

Ab Initio Calculations and Carbon-13 NMR Study on the Methoxymethyl Cation[1]

D. Fărcasiu* and J. A. Horsley*

Contribution from Exxon Research and Engineering Company, Corporate Research-Science Laboratories, Linden, New Jersey 07036. *Received August 8, 1979*

Abstract: The relative energies of several conformations of the title ion (**1**) have been computed by single configuration ab initio calculations with geometry optimization at both STO-3G and 4-31G level. The planar form **3** is the stable conformation, followed by the linear form **4**, which should represent the top of the barrier for the geometrical isomerization of **3**; the perpendicular form **5** is less stable. The high relative energy of the 1,3 hydrogen-bridged structure **7** agrees with experimental estimates for the barrier for 1,3-hydride shift in **1** in the gas phase. The perpendicular conformation **6**, with a C1–O–C3 angle equal to that in **7** is more stable than the latter but still lies far higher in energy than **5**, in which the C1–O–C3 angle was kept the same as in **3**. Both the energy sequencing and the variation of C1–O bond length in the series **3**, **4**, **5** parallel those calculated by previous authors for protonated formaldehyde (**2**). On the other hand, the response of the O–C3 bond length to the conformational changes in the series **3**, **5**, **6** parallels that calculated previously for the corresponding conformations of the 1-propyl cation (**8**), while the energy variations in the two series are opposite. From the calculated stabilization energies it is concluded that ion **1** is more stable than the 2-propyl cation, and even the perpendicular form **5** is more stable than the 1-propyl cation. The charge distribution calculated for all conformers suggests that oxygen in formaldehyde acquires an extra negative charge upon coordinating a methyl cation. Most of the positive charge in **1** is distributed among the hydrogen atoms; this is similar to what the calculations predict for ions **2** and **8**. Comparison of calculations on **1** and **2** suggests that replacement of H by CH_3 enhances the π donation from oxygen to carbon but has little effect upon the σ donation from carbon to oxygen. The relative energies, the bond lengths, and the orbital populations all indicate a significant hyperconjugation in **5**. Comparison with **8** suggests that O–C hyperconjugation is more effective than C–C hyperconjugation in stabilization of carbocations. Strong hyperconjugation alone can produce significant alterations of bond lengths. Formation of **1** from methoxyacetyl chloride (**19**) does not involve the corresponding acyl cation (**20**) as an intermediate stable at low temperature as reported in the literature. Instead, ^{13}C NMR supports the intermediacy of a halogen-coordinated complex of **19** with SbF_5 (**21**). The ^{13}C NMR spectrum of **1** has been recorded and is discussed in terms of the calculated charge distribution.

The methoxymethyl cation (**1**) is one of the few primary carbocations stable enough to be studied in super acid solutions,[2] as well as in the gas phase.[3] Yet, theoretical studies of ion **1** are scarce.[4] We have calculated the geometries and energies of various conformations of this cation, comparing the results with the existing experimental data. A comparison with calculations on protonated formaldehyde (**2**)[5] was also made.

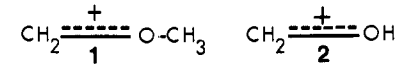

Calculations were carried out by using the ab initio SCF-MO Gaussian 70 programs.[6] The structures were first optimized at the STO-3G level.[7] The STO-3G geometries were then used as the starting point for a partial geometry optimization (one cycle) at the split-valence basis 4-31G level.[8] One optimization cycle

(1) Presented in part at the 177th National Meeting of the Americal Chemical Society, Honolulu, HI, Apr 1979; American Chemical Society, Washington, DC, 1979; Abstract No. ORGN 359.

(2) (a) Olah, G. A.; Bollinger, J. M. *J. Am. Chem. Soc.* **1967**, *89*, 2993. (b) White, A. M.; Olah, G. A. *Ibid.* **1969**, *91*, 2943.

(3) See for example: (a) Shannon, T. W.; McLafferty, F. W. *J. Am. Chem. Soc.* **1966**, *88*, 5021. (b) Harrison, A. G.; Ivko, A.; Van Raalte, D. *Can. J. Chem.* **1966**, *44*, 1625. (c) Haney, M. A.; Franklin, J. L. *Trans. Faraday Soc.* **1969**, *65*, 1794. (d) Beauchamp, J. L.; Dunbar, R. C. *J. Am. Chem. Soc.* **1970**, *92*, 1477. (e) Finney, C. D.; Harrison, A. G. *Int. J. Mass Spectrom. Ion Phys.* **1972**, *9*, 221. (f) McLafferty, F. W.; Kornfeld, R.; Haddon, W. F.; Levsen, K.; Sakai, I.; Bente, P. F., III; Tsai, S. C.; Schuddemage, H. D. R. *J. Am. Chem. Soc.* **1973**, *95*, 3886. (g) Dunbar, R. C.; Shen, J.; Melby, E.; Olah, G. A. *Ibid.* **1973**, *95*, 7200. (h) Hvistendahl, G.; Williams, D. H. *Ibid.* **1975**, *97*, 3097. (i) Schoemaker, M. E.; Nibbering, N. M. M.; Cooks, R. G. *Ibid.* **1975**, *97*, 4415. (j) Williams, D. H.; Bowen, R. D. *Ibid.* **1977**, *99*, 3192. (k) Bowen, R. D.; Williams, D. H.; Hvistendahl, G. *Ibid.* **1977**, *99*, 7509. (l) Smith, R. D.; Herold, D. A.; Elwood, T. A.; Futrell, J. *Ibid.* **1977**, *99*, 6042. (m) Losing, F. P. *Ibid.* **1977**, *99*, 7526.

(4) (a) Two semiempirical treatments have dealt with the charge distribution in a nonoptimized planar geometry of **1**: Nakano, S.; Iwasaki, K.; Fukutani, H. *J. Polym. Sci., A-1* **1963**, 3277. Eyzner, Yu. E.; Yerusalimskii, B. L. *Vysokomol. Soedin.* **1970**, *A12*, 1614. (b) See also: John, I. G.; Radom, L. *J. Mol. Struct.* **1977**, *36*, 133.

(5) (a) Ros, P. *J. Chem. Phys.* **1968**, *49*, 4902. (b) Haney, M. A.; Patel, J. C.; Hayes, E. F. *Ibid.* **1970**, *53*, 4105. (c) Purcell, K. F.; Collins, J. M. *J. Am. Chem. Soc.* **1970**, *92*, 465. (d) Lathan, W. A.; Curtiss, L. A.; Hehre, W. J.; Lisle, J. B.; Pople, J. A. *Prog. Phys. Org. Chem.* **1974**, *11*, 175. (e) Hopkinson, A. C.; Csizmadia, I. G. *Can. J. Chem.* **1974**, *52*, 546. (f) Bernardi, F.; Csizmadia, I. G.; Schlegel, H. B.; Wolfe, S. *Ibid.* **1975**, *53*, 1144. (g) Wolfe, S.; Schlegel, H. B.; Wangbo, M. H. *Ibid.* **1976**, *54*, 795. (h) Del Bene, J. E.; Vaccaro, A. *J. Am. Chem. Soc.* **1976**, *98*, 7526. Del Bene, J. E. *Ibid.* **1978**, *100*, 1673. (i) Bernardi, F.; Mangini, A.; Epiotis, N. D.; Larson, J. R.; Shaik, S. *Ibid.* **1977**, *99*, 7465. (j) Del Bene, J. E. *Chem. Phys. Lett.* **1978**, *55*, 235. (k) Wellington, C. A.; Khowaiter, S. H. *Tetrahedron* **1978**, *34*, 2183. (l) Schleyer, P. v. R.; Jemmis, E. D.; Pople, J. A. *J. Chem. Soc., Chem. Commun.* **1978**, 190.

(6) Hehre, W. J.; Lathan, W. A.; Ditchfield, R.; Newton, M. D.; Pople, J. A. *Program No. 236*, QCPE, Indiana University, Bloomington, Indiana, 1971.

(7) Hehre, W. J.; Stewart, R. F.; Pople, J. A. *J. Chem. Phys.* **1969**, *51*, 2657.

0002-7863/80/1502-4906$01.00/0